Published online November 27, 2005

Nucleic Acids Research, 2005, Vol. 33, No. 21 ***e182***
doi:10.1093/nar/gni181

Faster quantitative real-time PCR protocols may lose sensitivity and show increased variability

Chelsey Hilscher, Wolfgang Vahrson and Dirk P. Dittmer*

Department of Microbiology and Immunology and Lineberger Comprehensive Cancer Center, The University of North Carolina at Chapel Hill, NC, USA

Received July 19, 2005; Revised October 16, 2005; Accepted October 31, 2005

ABSTRACT

Quantitative real-time PCR has become the method of choice for measuring mRNA transcription. Recently, fast PCR protocols have been developed as a means to increase assay throughput. Yet it is unclear whether more rapid cycling conditions preserve the original assay performance characteristics. We compared 16 primer sets directed against Epstein–Barr virus (EBV) mRNAs using universal and fast PCR cycling conditions. These primers are of clinical relevance, since they can be used to monitor viral oncogene and drug-resistance gene expression in transplant patients and EBV-associated cancers. While none of the primers failed under fast PCR conditions, the fast PCR protocols performed worse than universal cycling conditions. Fast PCR was associated with a loss of sensitivity as well as higher variability, but not with a loss of specificity or with a higher false positive rate.

INTRODUCTION

Quantitative real-time PCR (QPCR) has rapidly become the method of choice for viral diagnosis and transcriptional analysis. Both absolute quantification and relative quantification methods by comparison between multiple primers have been developed (1–8). The widespread use of QPCR in viral diagnostics [reviewed in (5)] has started a wave of new developments, which claim to improve upon the standard protocols. Recently, fast cycling QPCR protocols have been developed. These cut the cycling time by as much as 50% relative to universal QPCR conditions (9). Here, we compare several rapid QPCR protocols with regard to sensitivity, specificity and false positive rate. This tests the hypothesis that an improvement in speed does not come at a loss of assay performance.

To compare the different protocols (Table 1), we used a set of 16 real-time QPCR primer pairs that recognized different mRNAs of Epstein–Barr virus (EBV). The target mRNAs are transcribed at different levels after chemical stimulation of EBV positive Burkitt's lymphoma cells (10) and are of clinical importance in gauging the response to antiviral drugs and tumor progression. This, rather than artificial substrates, best approximates 'real-world' conditions. The same cDNA pool was used for all experiments. We used random hexamers to prime the RT reaction. Therefore, the target mRNAs are present as a minor fraction in a pool of non-target mRNAs. Each primer pair was tested in triplicate for each cycling condition (Table 1) to yield mean cycle threshold (CT) and SD. We had shown previously that real-time QPCR based on SYBR green as the method of detection is as sensitive as TaqMan™ or probe-based assays if the primer pairs conform to TaqMan™ design parameters as defined in PrimerExpress™ v1.2 (11). All our primers were designed for an annealing temperature of 60°C and TaqMan™ assay conditions using ePrimer3 (7). We designed a group of experiments that use the same targets, primers, primer concentrations and PCR reagents to test the hypothesis that changes to fast PCR cycle parameters can be incorporated into existing protocols without changing reagents or primer concentration.

First, we tested universal cycling conditions (94°C for 15 s, 60°C for 60 s) and our previously described set-up (7) in three different experiments to establish plate-to-plate variation (16 primer pairs × triplicate measurements × 3 plates = 144 data points). Second, we tested fast cycling conditions variant 'Afast', which cut the assay time in half (Table 1) (16 primer pairs × triplicate measurements = 48 data points). Next, we tested cycling conditions variant 'Mfast' (16 primer pairs × triplicate measurements = 48 data points). These experiments used the same commercial QPCR mix. We typically analyze 100–400 different real-time QPCR primers pairs per day and therefore optimizing each primer pair concentration for each PCR condition or reagent mix individually is not a viable option. Since reagent makeup can affect assay performance, we also tested a second 2× SYBR mix and the manufacturer's fast PCR protocol. Lastly, we varied the annealing temperature to be either 60°C as used for universal cycling conditions or 62°C, which is recommended to improve

*To whom correspondence should be addressed. Tel: +1 919 966 7960; Fax: +1 919 962 8103; Email: ddittmer@med.unc.edu

Table 1. PCR conditions[a]

Name	Step 1 °C	s	Step 2 °C	s	Step 3 °C	s	Run time (min)
Conventional[b]	95	15	60	15	72	60	60
Universal	95	15	60	60	n/a[c]	n/a	50
Afast	95	1	64	35	n/a	n/a	24
Mfast	95	5	60	15	72	15	23
Sfast	95	10	60/62	30	n/a	n/a	26

[a]All protocols are preceded by an initial 5 min at 95°C step to activate the polymerase and repeated for 40 cycles.
[b]Conventional conditions are shown for comparison assuming an extension time of 60 s per 1000 bp amplicon length and optimal *Taq* polymerase activity at 72°C (7).
[c]Non applicable.

fast PCR assay performance (16 primer pairs × triplicate measurements = 48 data points at 60°C and 16 primer pairs × triplicate measurements = 48 data points at 62°C). This represents the type of adjustment that can easily be accommodated across many primers in routine operations.

MATERIALS AND METHODS

RNA isolation and RT

RNA was isolated from cell homogenates using the QiaQuick™ micro-prep kit (Quiagen Inc., Valencia, CA) and subjected to DNAse treatment using DNAfreeRNA™ kit (ZymoResearch Inc., Orange, CA) following the manufacturer's instructions. RT was performed as described previously (12). Briefly, 500 ng of RNA was reverse transcribed in a 20 µl reaction with 100 U of SuperscriptII reverse transcriptase (Invitrogen Inc., Carlsbad, CA), 2 mM deoxyribonucleoside triphosphates, 2.5 mM $MgCl_2$, 1 U of RNasin and 0.5 µg of random hexanucleotide primers (all from Applied Biosystems, Foster City, CA). The reaction mix was sequentially incubated at 42°C for 45 min, 52°C for 30 min and 70°C for 10 min. The RT reaction was stopped by heating to 95°C for 5 mins. Next, 0.5 U RNase H (Invitrogen Inc., Carlsbad, CA) were added, and the reaction incubated at 37°C for an additional 30 min and again heated to 95°C for 10 min. Afterwards, the cDNA pool was chilled on ice and diluted 25-fold (500 µl final volume) with diethyl pyrocarbonate-treated, distilled H_2O and stored at −80°C.

Real-time QPCR

The primers used in this study were derived from the human EBV genome and designed using the PrimeTime and TaqMan™ design criteria as published previously (7). They are ebv2, vil10; ebv15, ebna2; ebv26, bmrf1; ebv28, mta; ebv35, bllf2; ebv37, ebna3a; ebv40, ebna3c; ebv42, zta; ebv44, rta; ebv46, ebna1; ebv54, helicase; ebv57, exonuclease; ebv58, kinase; ebv72, bxrf1; ebv73, thymidine kinase; ebv78, bilf1; ebv79, polymerase; ebv83, barf1. The forward primer is designated '−1' and the reverse primer '−2'. The sequences are as follows: ebv2-1, CTGCCGTGTGAGAACAAGAG; ebv15-1, TGTGGTTGGGCAGGTACA; ebv26-1, CAACACCGCACTGGAGAG; ebv28-1, TACAACCCTGGCACGCTAA; ebv35-1, CCCGCTGGACTTTTACGA; ebv37-1, GAAGAGAAAGCGGGTCGAT; ebv40-1, AAGGTGCATTTACCCCACTG; ebv42-1, CTGCGCCTCCTGTTGAAG; ebv44-1, GAGTCCATGACAGAGGATTTGA; ebv46-1, TAGATTTGCCTCCCTGGTTT; ebv54-1, CCTCTACACCGCCGTCAC; ebv57-1, CATCCGTAAGACCTTGAGCA; ebv58-1, AAAAGAGGTTCAAGGAGAGCTAC; ebv72-1, AGAATTTAAGACGGCCATGAG; ebv73-1, GGACGATTTACCTGGATGCT; ebv78-1, TGGCCCTGTTGCTCATTAT; ebv79-1, GTGGCCGTGGATCATTATTT; ebv83-1, CAAATGGCGGTGTTATGAAG; ebv2-2, CACTCATGGCTTTGTAAATTCC; ebv15-2, CCCCATGTAACGCAAGATAG; ebv26-2, GCCTGCTTCACTTTCTTGG; ebv28-2, AGAGAATGGCCCTGACAAGT; ebv35-2, GCATGGAGAGGTTTGAGAATC; ebv37-2, GAAACCTGCGGAGAATGG; ebv40-2, AGCAGTAGCTTGGGAACACC; ebv42-2, TTAAGAGATCCTCGTGTAAAACATCT; ebv44-2, GCAGCAGACATTCATCATTTAGA; ebv46-2, ACCCTCATCTCCATCACCTC; ebv54-2, ACAAAGCCCAGGATGAACTC; ebv57-2, GTCGGCAAAGAGACCAGAG; ebv58-2, AGTCGTCTGCCAAGAGTTCA; ebv72-2, TTGGCACAGTCACACAACTG; ebv73-2, TCAGAGATCACCTTGCTCAGA; ebv78-2, TCTGAAGTATCTGGCGGTGA; ebv79-2, AAAATTCTGGAGGACGGAGA; and ebv83-2, TTCCCAACGCAGGTCACT.

Real-Time PCR was conducted according to previously established procedures (7). The final PCR mixture contained 10 µl of combined forward and reverse primers (final concentration of each, 166 nM), 15 µl of 2× SYBR PCR mix (Applied Biosystems, Foster City, CA or Stratagene Inc., La Jolla, CA), and 5 µl of sample. Real-time PCR was performed with an MJR Opticon 2 unit under the indicated cycling conditions (Table 1). CT values were determined by automated threshold analysis (3× SD of the global minimum across all primers and samples in a plate). PCR was set up in a dedicated room using the CAS-1200 pipetting robot (Corbett Research Inc., Australia). The CAS-1200 robot uses filtered carbon-graphite pipette tips (Tecan Inc., Durham, NC) for liquid level sensing, allowing for a pipetting accuracy of 0.1 µl, and elimination of carry-over contamination. All surfaces were cleaned with 10% bleach weekly, and exposed to UV lights overnight. Designated gowns, gloves and facemasks were required for all work. Dissociation curves were recorded after each run and the amplified products were visualized by 2% agarose gel electrophoresis. Analysis of dissociation profiles was performed with MJR Opticon 2 software (MJR Inc., Boston, MA), which calculated the melting temperature (T_m) for each reaction.

Statistical analysis

Calculations were performed using Excel v10.1 (Microsoft Inc., Redwood WA) and SPSS v12.0 (SPSS science, Chicago, IL) under MacOS v10.3.9. Further calculations were conducted using Mathematica v5.0 (Wolfram Research, Champaign, IL).

RESULTS

Impact on false-positive rate

To determine whether faster QPCR protocols increased the false-positive rate, i.e. yield a signal in the non-template control (NTC) reaction, we performed a NTC PCR for each primer pair (n = 16). The NTC results were expected to equal the

Table 2. Summary of CT data for NTCs[a]

Protocol	*N*	Minimum	Maximum	Mean	SEM	SD
Universal	16	35.29	40.00	39.39	0.35	1.39
Universal	16	36.10	40.00	39.41	0.32	1.28
Universal	16	35.73	40.00	39.06	0.42	1.70
Afast	16	36.99	40.00	39.81	0.19	0.75
Mfast	16	40.00	40.00	40.00	0.00	0.00
Sfast at 60°C	16	27.02	40.00	34.54	0.83	3.32
Sfast at 62°C	16	30.60	40.00	35.67	0.70	2.79

[a]Amplification reaction of the NTC.

maximal cycle number independent of any particular primer pair. The result is presented in Table 2. A positive signal in the NTC reaction can be due to primer dimer formation and subsequent SYBR green intercalation, secondary structures resulting in stems, non-specific addition of nucleotides by the *Taq* polymerase (which is the basis for TA-cloning), or contamination with a positive target. Even though most primer design programs eliminate the obvious secondary structures, depending on the salt conditions any polynucleotide >20 bases will form some secondary structure to which intercalating dyes may bind (13). The mean NTC signal was identical to the maximal cycle number ($CT_{max} = 40$) for all conditions using the ABI master mix. The NTC signal using the Stratagene mix and cycling conditions was ~5 cycles lower, but in most instances so was the positive CT signal (see below). However, the variation in the NTC under these conditions was excessive with a maximal SD of 3.32 cycles compared with a maximal SD of 1.70 cycles for all other conditions. The Mfast conditions never yielded any signal in the NTC, but also had the lowest sensitivity overall (see below). There was no significant difference in the mean CT signal for the NTC reaction using universal or Afast or Mfast cycling conditions, demonstrating that these faster cycling protocols were not associated with a higher false-positive rate or loss of specificity.

Impact on sensitivity and false negative rate

To determine whether faster QPCR protocols are associated with a loss of sensitivity, we determined the mean CT for each primer pair under each cycling protocol (Figure 1). Because the target mRNAs for each primer pair are present at different levels during natural EBV reactivation, we used the same input cDNA pool representing several log step variation of target levels in a background of non-target molecules. This approximated real-world conditions for viral load and transcriptional profiling applications. The Afast and Mfast cycling protocols were less sensitive across all primer pairs compared with universal cycling conditions and also were associated with higher variability (Figure 1A). Given the same amount of input cDNA these protocols yielded higher CT values for each primer pair. The Sfast protocol and reagents were more sensitive than universal cycling conditions, yielding a lower CT value for the same input cDNA pool. Across all primers, universal cycling conditions yielded a mean CT ± SD ($n = 48$) of 30.22 ± 3.21, 30.83 ± 3.09 and 30.00 ± 2.96 for three consecutive runs. The Afast conditions yielded 37.32 ± 2.76, the Mfast conditions 36.11 ± 3.09. The Sfast conditions at 60°C annealing temperature yielded a mean CT ± SD of 28.60 ± 3.36 and at 62°C annealing temperature a mean CD ± SD of 28.81 ± 3.90. Hence, increasing the annealing temperature 2°C above the calculated T_m did not lower the sensitivity. This was also true under universal cycling conditions (data not shown). Figure 1B depicts the variation in three replicate runs using universal cycling conditions compared with Afast cycling conditions. In each case the fast cycling conditions were associated with a significant loss in sensitivity. As expected, the results for each of the protocols and primers were highly correlated (Figure 1C and Table 3). Replicates under identical cycling conditions were more highly correlated than between different cycling conditions. The standardized slope of the linear regression between two universal cycling assays, #2 and #3, was $m = 0.974$ with a 90% confidence interval of 0.944–1.083 and $R^2 = 0.949$. Relative to universal cycling conditions (#2), the Sfast conditions at both temperatures shifted CT values by a fixed difference to the left but with the same slope. The same primer yielded a lower CT for the same target. This suggests that the Stratagene dye formulation was brighter, but the PCR efficiency was the same. Relative to universal cycling conditions (#2) the Afast and Mfast conditions shifted the CT values to the right and at the same time lowered the slope. The same primer yielded a higher CT for the same target and low target concentrations yielded disproportional higher CT values. This indicated of a loss of amplification efficiency, i.e. a loss of sensitivity, for the Afast and Mfast QPCR protocols compared with universal cycling conditions.

Impact on reproducibility

To determine whether faster QPCR protocols were associated with a loss in reproducibility, we determined the SDs in CT for each primer pair under each cycling protocol in Table 1. In a separate experiment, we first determined the total variation associated with our experimental set-up, which uses a pipetting robot and filtered liquid-sensing tips, and 30 µl total reaction volume. Based on $N = 64$ replicates of a real-world cDNA sample (mean CT: 20.57) under universal cycling conditions we determined the SD, 0.72 cycles; SEM, 0.09 cycles; and CV, 3.5%. The associated T_m was 82.2°C with SD, 0.19°C; SEM, 0.24°C; and CV, 0.23% (Figure 2).

For each of the real-time PCR cycling conditions, we first calculated the SD of amplification for each primer pair separately ($n = 3$) and determined the statistics of the SD's for each primer pair across all PCR cycling conditions ($n = 7$) and across all primer pairs for each PCR cycling condition ($n = 16$). These are depicted as box plots in Figure 3A and B. This represents the most relevant statistic for routine applications of QPCR, because different primer pairs perform with different amplification efficiencies and are used against a range of target concentrations within the total cDNA pool. All primers were at the same concentration and on the same physical plate. We performed three repeats of the universal cycling conditions (#1, #2 and #3), to determine the run-to-run variation. Across all primer pairs universal cycling conditions yielded the most consistent results with mean CT SDs of 0.52, 0.40 and 0.47, respectively. Outliers resulted from PCR failures within a single primer triplicate ($CT = CT_{max}$), which have a disproportional effect on the SD. Hence, excluding results with $CT = CT_{max}$ would be an

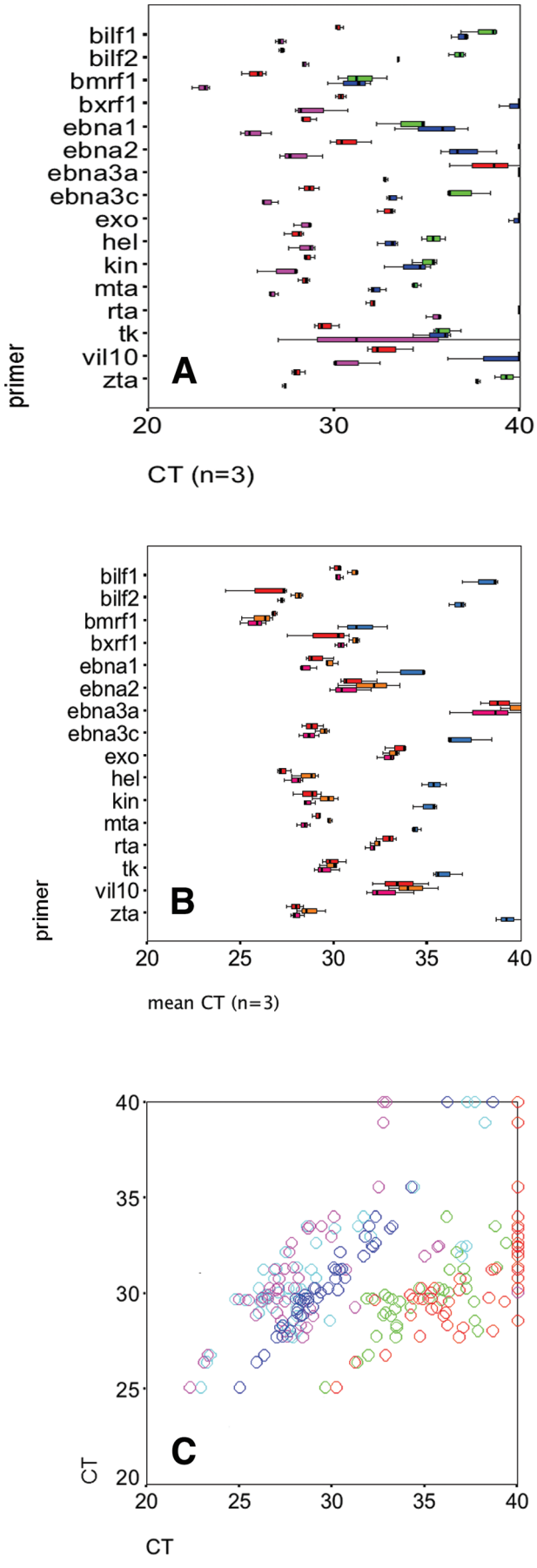

appropriate rule to reduce false negative results, since it cannot be decided whether such an outcome was due to the absence of target or instrument/pipetting error in the particular well.

The faster PCR cycling protocols were associated with increased variability for each primer pair with mean SD ($N = 16$) for Afast, 0.54; Mfast, 0.71; Sfast60, 1.57. An exception was Sfast62 with a mean SD of 0.41. Independent of individual primer efficiency or target abundance, faster PCR cycling conditions resulted in higher variability. The quartile ranges (Figure 3B) for any of the fast PCR cycling protocols were higher than even the worst replicate under universal cycling conditions.

All primers, which were designed to comply with universal cycling conditions ($T_m = 60°C$) performed under all conditions. Using paired *t*-test and Pearson's correlation analysis we did not find significant differences in either the primer pairs or PCR conditions (data not shown). However, raising the annealing temperature from 60 to 62°C lowered sample-to-sample variation (Figure 3B). Similarly, using universal cycling conditions we found that raising the annealing temperature to 62°C ($n = 8$ primers with a calculated T_m of 60°C) also lowered sample-to-sample variation without loss of sensitivity. Only if the annealing temperature was raised to 64°C and above did we observe a loss in sensitivity (one cycle) for these primers (data not shown).

Robustness as a new criterion for primer design

Different primer pairs exhibited different degrees of variation in SD of triplicate measurements across the various PCR cycling conditions (Table 4). This can be used as an additional quality control criterion for primer design. Sensitivity and specificity being equal, a 'robust' primer pair will yield lower variation (defined as 75% quartile range) in SD across a range of conditions and reagents. The SD for each primer pair did not correlate with target concentration under any condition with a minimal $P \geqslant 0.05$ using Pearson's correlation analysis (data not shown), which recapitulates our earlier findings on a set of $n = 96$ different primer pairs (7,11). Primers BILF1 [meanCT(#3) = 30.28], BILF2 [meanCT(#3) = 27.19], EBNA3C [meanCT(#3) = 28.67], Exo [meanCT(#3) = 33.24], HEL [meanCT(#3) = 28.33], MTA [meanCT(#3) = 28.69] had the lowest variation in SD across the different PCR cycling conditions. This establishes that primer 'robustness' across different PCR conditions is independent of sensitivity and specificity.

All QPCR protocols yielded outliers, i.e. extremely high SD for a particular primer pair (Figure 3B). This suggests that different PCR cycling conditions put different constraints on primer performance that are not captured by the theoretical design parameters for universal cycling conditions. Of note, all

Figure 1. (**A**) CT values across $n = 16$ primer pairs for different QPCR conditions: universal (red), Afast (green), Mfast (blue) and Sfast at 60°C (purple) (**B**) CT values across $n = 16$ primer pairs for different QPCR conditions: universal repeat #1, universal repeat #2, universal repeat #3 (all shades of red) and Afast (blue). The box represents the interquartile range, whiskers indicate the highest and lowest values, excluding outliers for triplicate measurements. A line across the box indicates the median. (**C**) Correlation of mean CT values for the indicated QPCR conditions relative to universal repeat #2 on the vertical axis: red, Afast; green, Mfast; blue, universal repeat #2; purple, Sfast at 60°C; light blue, Sfast at 62°C.

Table 3. Correlations between cycling protocols over all primers

Protocol	Measure	#1	#2	#3	Afast	Mfast	Sfast60°	Sfast62°
Universal	Pearson[a]	1	0.956	0.955	0.614	0.714	0.554	0.808
	Sigma[b]		4.38E−26	7.16E−26	3.44E−06	1.18E−08	4.44E−05	3.81E−12
Universal	Pearson		1	0.974	0.672	0.741	0.572	0.811
	Sigma			1.97E−31	1.67E−07	1.75E−09	2.20E−05	2.67E−12
Universal	Pearson			1	0.688	0.768	0.592	0.839
	Sigma				6.50E−08	1.96E−10	9.30E−06	9.70E−14
Afast	Pearson				1	0.84	0.526	0.704
	Sigma					8.12E−14	1.25E−04	2.37E−08
Mfast	Pearson					1	0.605	0.752
	Sigma						5.25E−06	7.45E−10
Sfast 60	Pearson						1	0.76
	Sigma							3.63E−10
Sfast 62	Pearson							1

[a]Pearson Correlation coefficient ($n = 48$).
[b]Sigma (P-value) for two-tailed t-test ($n = 48$).

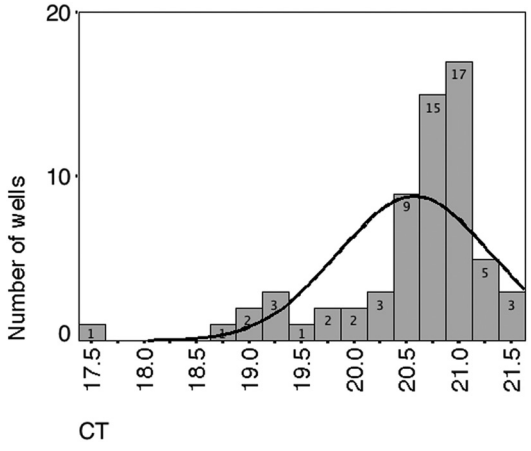

Figure 2. Variation based on pipetting and instrument error. Depicted is a histogram for the CT values obtained from $n = 64$ replicates. The vertical axis shows the number of wells and the horizontal axis the CT values. The calculated normal distribution is overlaid in black.

primer pairs used here yielded amplicons of size 100 ± 25 bp, which is well below the estimated *Taq* polymerase extension rate of 1000 bp per 60 s (14). Hence, primer robustness was dependent on the flanking primers, not the length of the amplicon. One can conjecture, however, that PCR primer pairs that generate larger amplicons are associated with high failure rates under rapid PCR cycling conditions, since fewer amplicons are completed per cycle.

One concern to this study could be that the number of primer pairs was too small to yield general conclusions. We therefore repeated the experiments using an additional $n = 85$ previously described primer pairs (7,12). These primer pairs yielded amplicons with a mean length of 63.11 bp, %CV = 0.27 bp and a calculated T_m of 60 ± 1°C. The mean K_{eff} of this primer set was 1.9025 with %CV = 0.0071. Since every primer pair in every primer set was within the open reading frame of a single copy viral or human gene, we used total cell DNA as the universal target in all experiments. Figure 4 plots the CT resulting from the same target under universal, Afast, Mfast and Sfast fast cycling conditions using the same reagent mix. Corroborating our prior observations, none of the fast PCR

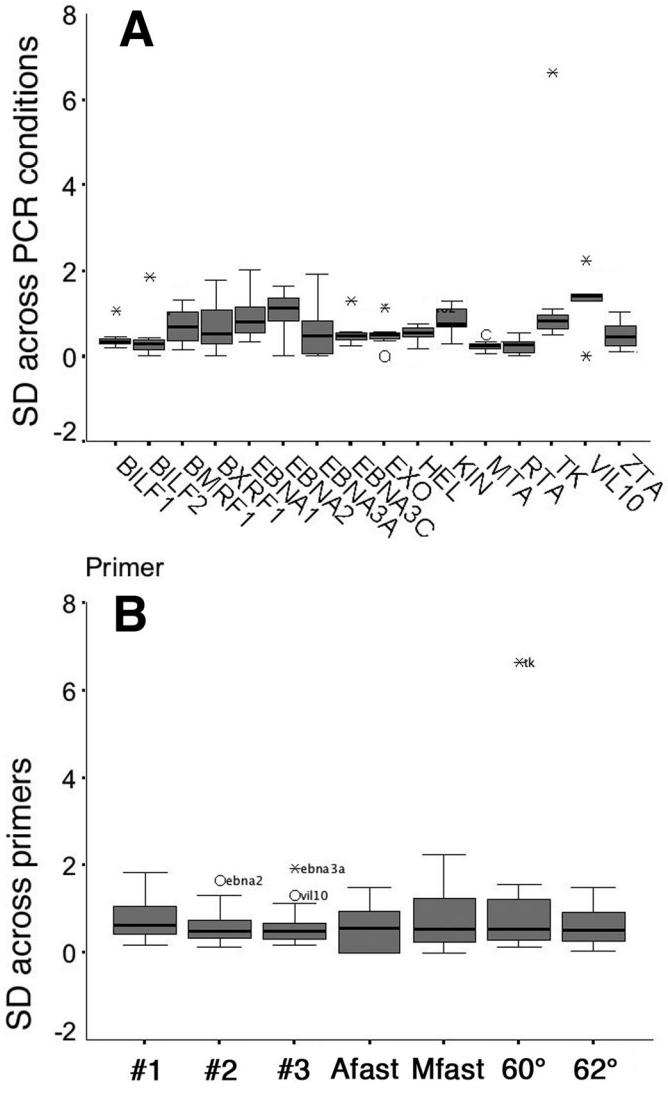

Figure 3. (**A**) SD across $n = 16$ primer pairs for each of the different QPCR conditions. (**B**) SD across $n = 7$ QPCR conditions for each of the 16 primer pairs. The box represents the interquartile range, whiskers indicate the highest and lowest values, excluding outliers. Asterisks indicate outliers. A line across the box indicates the median.

Table 4. Comparison of SD across primers and conditions

Primer	Universal 1, 2, 3			Afast	Mfast	Sfast60	Sfast62	*n*	Mean	Median	SEM	SD
bilf1	0.33	0.30	0.20	1.06	0.47	0.29	0.36	7	0.43	0.33	0.11	0.29
bilf2	1.84	0.33	0.15	0.44	0.02	0.16	0.27	7	0.46	0.27	0.24	0.62
bmrf1	0.16	0.88	0.68	1.33	1.20	0.50	0.26	7	0.72	0.68	0.17	0.45
bxrf1	1.78	0.30	0.29	0.00[a]	0.65	1.55	0.52	7	0.73	0.52	0.26	0.68
ebna1	0.78	0.35	0.47	1.49	2.02	0.85	0.63	7	0.94	0.78	0.23	0.60
ebna2	1.04	1.64	1.13	0.00[a]	1.55	1.21	0.59	7	1.02	1.13	0.22	0.57
ebna3a	1.06	0.61	1.92	0.00[a]	0.00[a]	0.10	0.48	7	0.59	0.48	0.26	0.70
ebna3c	0.58	0.40	0.54	1.30	0.40	0.47	0.25	7	0.56	0.47	0.13	0.34
exo	0.59	0.45	0.50	0.00[a]	0.36	0.54	1.13	7	0.51	0.50	0.13	0.33
hel	0.37	0.74	0.54	0.64	0.54	0.76	0.19	7	0.54	0.54	0.08	0.21
kin	0.75	0.72	0.31	0.69	1.30	1.22	1.01	7	0.86	0.75	0.13	0.35
mta	0.24	0.11	0.34	0.25	0.49	0.26	0.04	7	0.25	0.25	0.06	0.15
rta	0.56	0.29	0.27	0.00[a]	0.00[a]	0.42	0.16	7	0.24	0.27	0.08	0.21
tk	0.64	0.50	0.68	0.81	1.11	6.64	0.83	7	1.60	0.81	0.84	2.23
vil10	1.48	1.31	1.31	0.00[a]	2.22	1.42	1.47	7	1.32	1.42	0.25	0.66
zta	0.46	0.77	0.37	0.67	0.12	0.11	1.04	7	0.51	0.46	0.13	0.34
n	16	16	16	16	16	16	16					
Mean	0.79	0.61	0.61	0.54	0.78	1.03	0.58					
Median	0.62	0.48	0.48	0.54	0.52	0.52	0.50					
SEM	0.13	0.10	0.12	0.13	0.18	0.39	0.10					
SD	0.52	0.40	0.47	0.54	0.71	1.57	0.41					

Gray shading indicates SD > 1 CT unit.
[a]Failure to amplify: CT = 40 for each of the triplicate sample wells.

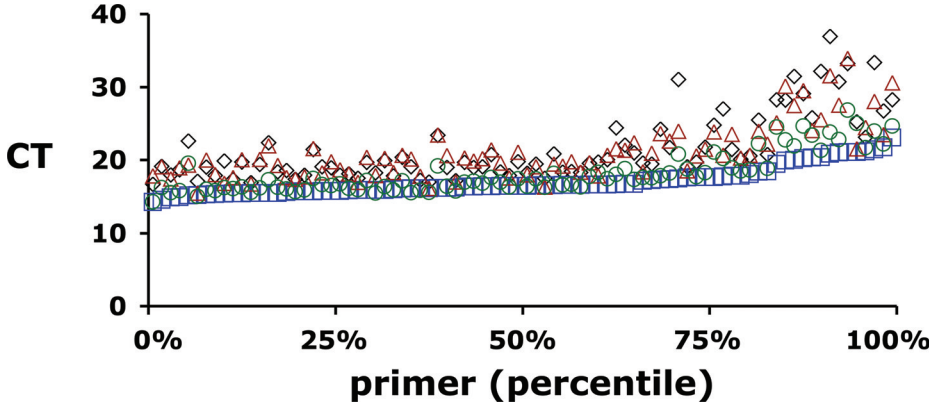

Figure 4. The vertical axis shows CT values for $n = 85$ primers using a total cellular DNA as template. The horizontal axis plots each primer as the percentile of the primer set that was rank-ordered based upon CT under universal cycling conditions. Blue squares show the result under universal cycling conditions at 60°C, green circles under Sfast at 62°C, red triangles under Mfast at 60°C and black rhombi under Afast conditions at 60°C.

cycling protocols was more sensitive than universal cycling conditions. None of the 85 primer pairs yielded a lower CT under any fast PCR protocol than under universal cycling conditions (blue squares). However, the Sfast protocol at 62°C annealing temperature was almost as sensitive as universal cycling conditions at 60°C. This was expected as it had the longest denaturation step and the second longest extension phase among the fast PCR protocols tested herein (Table 1).

Given a fixed, identical amount of total DNA as target in each reaction, all primer pairs were expected to yield the same CT. Variability in CT values between different primers was introduced owing to pipetting inaccuracies and differences in primer efficiency. The mean ± SEM CT of the $n = 85$ primer set under universal conditions was 17.00 ± 0.21 (%CV = 11.59). It increased to 18.14 ± 0.31 (%CV = 15.60) for Sfast at 62°C, 20.85 ± 0.41 for Mfast and 21.37 ± 0.49 (%CV = 21.30%) for the Afast cycling protocol. Not only did the sensitivity drop (as indicated by increased meanCT), but the variation between primers (as indicated by SEM) increased under fast PCR conditions. This corroborates the prior results in Figure 3.

The top 50% of primers (those with near ideal amplification efficiencies) showed the least performance loss under fast PCR conditions. Comparing the SD for all $n = 85$ primer pairs across all PCR conditions yielded a mean SD of 2.26 ± 0.15. The mean SD for the top 43 primer pairs across all PCR conditions was 1.76 ± 0.11, while the mean SD for the bottom 42 primer pairs across all PCR conditions was 2.77 ± 0.26 (Figure 4). This corroborates the initial experiments in a larger primer set and emphasizes the utility of primer 'robustness' across multiple PCR cycling conditions as an additional measure of performance and criterion for primer design.

DISCUSSION

As QPCR becomes ever more popular, so does the need for high-throughput analysis. One approach to this bottleneck is represented by the development of fast cycling protocols, which cuts the time of each QPCR run roughly by half (Table 1). Here, we explored whether the faster cycling protocols were associated with a loss of sensitivity, loss of specificity or increase in variability. One caveat of our analysis was that we used the same reagents under all different cycling conditions. This was necessary to adequately compare the conditions with each other. This experimental design yields a lower bound estimate of overall performance. Using the manufacturer's recommended fast-cycling reagents and optimizing each primer pair for each condition may improve sensitivity and reproducibility. Increasing the annealing temperature from 60 to 62°C increased performance for primers with a predicted T_m of 60°C regardless of the PCR conditions. Perhaps increasing the primer concentrations for fast PCR cycling protocols relative to optimal concentrations, as determined under universal cycling conditions, would increase sensitivity as well. However, in our experience higher primer concentrations while at times associated with increased sensitivity, were also associated with a loss in specificity and higher background signal in the NTC reaction, i.e. an increase in the false positive rate (data not shown). This re-emphasizes that changes in primer concentration exert a non-linear, bell-shaped response on PCR performance and require extensive experimental optimization for each and every primer. Without optimization, fast QPCR cycling conditions performed worse than universal cycling conditions. All fast QPCR protocols were associated with a loss of sensitivity and higher variability, although they retained target specificity and similar false positive rates compared with universal cycling conditions.

We purposefully conducted all experiments on a single real-time QPCR instrument. This experimental design eliminated any and all variation owing to mechanical imprecision between different units. However it leaves this study open to criticism that QPCR units by other manufacturers may perform better. Indeed, specialized 'fastPCR' machines are available. In case of the Roche Lightcycler, a specialized set of reagent vessels are required to achieve fast cycling times. In contrast all other real-time QPCR units that accept standard 96well formats use the same Peltier-based technology. Of the four fast cycling PCR protocols that we evaluated one protocol matched our machine and it performed no better than protocols developed for QPCR machines by other manufacturers. But all other protocols were designed to be machine independent. Two factors are routinely cited as essential for fast PCR (i) a modified hot-start polymerase that is more rapidly activated at 95°C and (ii) a faster ramp time of ⩾3.5°C/s. Since all PCR protocols compared here were preceded by a 95°C/5 min activation step (Table 1) the polymerases were fully and equally active before the first cycle starts for each protocol. Ramp speed indeed represents a machine-dependent variable. Older units typically have a ramp speed of <2.0°C/s. The MJR Opticon 2 has a ramp speed of 3.0°C/s, which approaches that of the designated fast PCR units. While a slower ramp speed will extend the total run time, we speculate that if anything, it should have a positive effect on sensitivity and variability, since more time is provided to reach the desired reaction temperatures. All PCR machines are designed such that the cycle timer for the next segment only starts after the desired temperature has been reached.

We predict that the time to reach equilibrium at the annealing step will impact QPCR efficiency, which can be thought of as the fraction of bi-molecular reactions that reach equilibrium ([primer-target] × K_{eq} = [primer] × [target]). This process is time dependent such that at μM concentrations base pairs have an intrinsic formation rate of $\sim 10^3$ per second (13). In fact, one manufacturer recommended to extend the annealing temperature, should poor amplification be encountered. This is corroborated by our finding (Figure 4) that primers of PCR lower efficiency under universal PCR conditions perform worse under fast PCR conditions than primers with high PCR efficiency under universal cycling conditions. Figure 5A depicts the relationship between cycle number CT, amplification efficiency K and total number of molecules. At $K = 1.7$, 40 cycles are needed to reach maximal amplification (8×10^8), while at $K = 2$ only 30 cycles are needed. Figure 5B shows the fold differential between ideal conditions

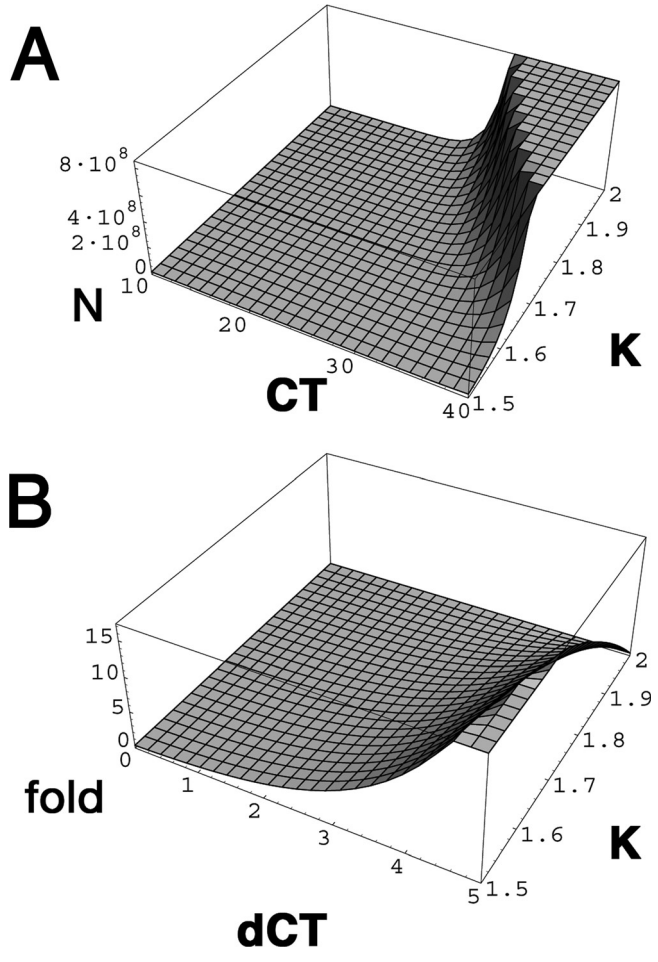

Figure 5. (**A**) Amplification dependence on amplification efficiency K. The X-axis shows cycle number CT, the Y-axis amplification efficiency K and the Z-axis the number of molecules starting from $N_0 = 1$. (**B**) Fold difference = $2^{dCT} - K^{dCT}$ shows the fold error (Z-axis) introduces by change in amplification efficiency K (Y-axis) for given dCT differences (X-axis).

$K = 2$ and different amplification efficiencies K. At $K = 1.7$ a dCT = 5 cycle difference, which is ~5× SD of most primers and most protocols evaluated here, between any two samples results in a 15-fold underestimate of the fold difference relative to $K = 2.0$. Hence, increasing the PCR efficiency by better primer design or slower QPCR conditions may yield a significant increase in sensitivity.

With regard to basic PCR amplification, we did not have to redesign any primer pair as none failed to amplify altogether under the new conditions. However, some existing primer-pairs did show a dramatic loss of performance under these cycling protocols while others performed with equal robustness regardless of the cycling parameters. Switching to fast PCR cycling protocols doubled our overall sample throughput. Therefore, the question remains whether the increased speed is worth the effort of optimizing each real-time PCR assay for fast PCR cycling protocols. Is it worth the down-time and set-up cost associated with optimizing primer concentration and annealing temperature all over again? Is it worth paying a premium for fast PCR optimized reagents? If only a single primer pair is used on many samples, such as in HIV viral load assays (15,16), this would be our recommendation. If many primer pairs are used and only on a relative limited number of samples, such as to profile transcription or to confirm microarray results (2), this would not be justifiable.

ACKNOWLEDGEMENTS

The authors thank Andrea Chaput for critical reading. This work was supported by NIH grants CA110136, EB00983 and CA109232 to D.P.D. Funding to pay the Open Access publication charges for this article was provided by NIH CA109232.

Conflict of interest statement. None declared.

REFERENCES

1. Jebbink,J., Bai,X., Rogers,B.B., Dawson,D.B., Scheuermann,R.H. and Domiati-Saad,R. (2003) Development of real-time PCR assays for the quantitative detection of Epstein–Barr virus and cytomegalovirus, comparison of TaqMan probes, and molecular beacons. *J. Mol. Diagn.*, **5**, 15–20.
2. Dittmer,D.P. (2003) Transcription profile of Kaposi's sarcoma-associated herpesvirus in primary Kaposi's sarcoma lesions as determined by real-time PCR arrays. *Cancer Res.*, **63**, 2010–2015.
3. Vandesompele,J., De Preter,K., Pattyn,F., Poppe,B., Van Roy,N., De Paepe,A. and Speleman,F. (2002) Accurate normalization of real-time quantitative RT–PCR data by geometric averaging of multiple internal control genes. *Genome Biol.*, **3**, RESEARCH0034.
4. Pfaffl,M.W., Horgan,G.W. and Dempfle,L. (2002) Relative expression software tool (REST) for group-wise comparison and statistical analysis of relative expression results in real-time PCR. *Nucleic Acids Res.*, **30**, e36.
5. Mackay,I.M., Arden,K.E. and Nitsche,A. (2002) Real-time PCR in virology. *Nucleic Acids Res.*, **30**, 1292–1305.
6. Pfaffl,M.W. (2001) A new mathematical model for relative quantification in real-time RT–PCR. *Nucleic Acids Res.*, **29**, E45–E45.
7. Papin,J., Vahrson,W., Hines-Boykin,R. and Dittmer,D.P. (2004) Real-time quantitative PCR analysis of viral transcription. *Methods Mol. Biol.*, **292**, 449–480.
8. Schmittgen,T.D., Jiang,J., Liu,Q. and Yang,L. (2004) A high-throughput method to monitor the expression of microRNA precursors. *Nucleic Acids Res.*, **32**, e43.
9. Heid,C.A., Stevens,J., Livak,K.J. and Williams,P.M. (1996) Real time quantitative PCR. *Genome Res.*, **6**, 986–994.
10. Kurokawa,M., Ghosh,S.K., Ramos,J.C., Mian,A.M., Toomey,N.L., Cabral,L., Whitby,D., Barber,G.N., Dittmer,D.P. and Harrington,W.J.,Jr (2005) Azidothymidine inhibits NF-kappaB and induces Epstein–Barr virus gene expression in Burkitt lymphoma. *Blood*, **106**, 235–240.
11. Papin,J.F., Vahrson,W. and Dittmer,D.P. (2004) SYBR green-based real-time quantitative PCR assay for detection of West Nile Virus circumvents false-negative results due to strain variability. *J. Clin. Microbiol.*, **42**, 1511–1518.
12. Fakhari,F.D. and Dittmer,D.P. (2002) Charting latency transcripts in Kaposi's sarcoma-associated Herpesvirus by whole-genome real-time quantitative PCR. *J. Virol.*, **76**, 6213–6223.
13. Cantor,C.R. and Schimmel,P.R. (1980) *Biophysical Chemistry: The Behavior of Biological Macromolecules*. Freeman, NY.
14. Innis,M.A., Gelfand,D.H., Sninsky,J.J. and White,T.J. (1990) *PCR Protocols*. Academic Press, NY.
15. Desire,N., Dehee,A., Schneider,V., Jacomet,C., Goujon,C., Girard,P.M., Rozenbaum,W. and Nicolas,J.C. (2001) Quantification of human immunodeficiency virus type 1 proviral load by a TaqMan real-time PCR assay. *J. Clin. Microbiol.*, **39**, 1303–1310.
16. Damond,F., Descamps,D., Farfara,I., Telles,J.N., Puyeo,S., Campa,P., Lepretre,A., Matheron,S., Brun-Vezinet,F. and Simon,F. (2001) Quantification of proviral load of human immunodeficiency virus type 2 subtypes A and B using real-time PCR. *J. Clin. Microbiol.*, **39**, 4264–4268.